J. Cell. Mol. Med. Vol 20, No 9, 2016 pp. 1749-1760

Methylglyoxal induces cell death through endoplasmic reticulum stress-associated ROS production and mitochondrial dysfunction

Chi-Ming Chan [a, b, c], Duen-Yi Huang [a], Yi-Pin Huang [d], Shu-Hao Hsu [d], Lan-Ya Kang [a], Chung-Min Shen [e, *], Wan-Wan Lin [a, f, *]

[a] Department of Pharmacology, College of Medicine, National Taiwan University, Taipei, Taiwan
[b] Department of Ophthalmology, Cardinal Tien Hospital, New Taipei City, Taiwan
[c] School of Medicine, Fu Jen Catholic University, New Taipei City, Taiwan
[d] Medical Research Center, Cardinal Tien Hospital, New Taipei City, Taiwan
[e] Department of Pediatrics, Cathay General Hospital, Taipei, Taiwan
[f] Graduate Institute of Medical Sciences, Taipei Medical University, Taipei, Taiwan

Received: February 4, 2016; Accepted: May 3, 2016

Abstract

Diabetic retinopathy (DR) and age-related macular degeneration (AMD) are two important leading causes of acquired blindness in developed countries. As accumulation of advanced glycation end products (AGEs) in retinal pigment epithelial (RPE) cells plays an important role in both DR and AMD, and the methylglyoxal (MGO) within the AGEs exerts irreversible effects on protein structure and function, it is crucial to understand the underlying mechanism of MGO-induced RPE cell death. Using ARPE-19 as the cell model, this study revealed that MGO induces RPE cell death through a caspase-independent manner, which relying on reactive oxygen species (ROS) formation, mitochondrial membrane potential (MMP) loss, intracellular calcium elevation and endoplasmic reticulum (ER) stress response. Suppression of ROS generation can reverse the MGO-induced ROS production, MMP loss, intracellular calcium increase and cell death. Moreover, store-operated calcium channel inhibitors MRS1845 and YM-58483, but not the inositol 1,4,5-trisphosphate (IP3) receptor inhibitor xestospongin C, can block MGO-induced ROS production, MMP loss and sustained intracellular calcium increase in ARPE-19 cells. Lastly, inhibition of ER stress by salubrinal and 4-PBA can reduce the MGO-induced intracellular events and cell death. Therefore, our data indicate that MGO can decrease RPE cell viability, resulting from the ER stress-dependent intracellular ROS production, MMP loss and increased intracellular calcium increase. As MGO is one of the components of drusen in AMD and is the AGEs adduct in DR, this study could provide a valuable insight into the molecular pathogenesis and therapeutic intervention of AMD and DR.

Keywords: methylglyoxal • ER stress • retinal pigment epithelium • mitochondria • reactive oxygen species • intracellular calcium

Introduction

The retinal pigment epithelium (RPE) is a component of the outer blood–retinal barrier (BRB) and carries out several important functions for the maintenance of the visual system. RPE cells are believed to play a crucial role for the pathogenesis of diabetic retinopathy (DR) [1] and age-related macular degeneration (AMD) [2]. DR is a common complication of diabetes mellitus (DM) and is the leading cause of acquired blindness in people aged 20–79 years [3]. On the other hand, AMD is the most common cause of visual impairment in individuals over the age of 55 years in developed countries [4] with characterized accumulation of lipid- and protein-rich deposits under the aged RPE that renders oxidant injury and heralds the onset of early AMD [5]. Much evidence indicates that hyperglycaemia is not only a primary factor in the development of DR, but also an important contributor to AMD [6]. Chronic exposure of the retina to hyperglycaemia gives rise to accumulation of advanced glycation end products (AGEs) in RPE basement membrane that plays an important role in

*Correspondence to: Dr Wan-Wan LIN, Ph.D.
E-mail: wwllaura1119@ntu.edu.tw

Dr Chung-Min SHEN
E-mail: shen8471@yahoo.com.tw

doi: 10.1111/jcmm.12893

both DR [7] and AMD [6, 8]. AGEs formation is a natural function of ageing, and AGEs act as mediators of neurodegeneration during ageing and AMD. AGEs-modified proteins that are highly formed in diabetic patients are also components of drusen, the sub-RPE deposits that confer increased risk of AMD onset [9]. Moreover, the receptor for AGEs (RAGE) is ubiquitously expressed in various retinal cells and is up-regulated in the retinas of diabetic patients [10] and in RPE cells associated with basal deposits occurring in AMD [11].

Methylglyoxal (MGO) is formed by various biochemical pathways and is present under normal physiological conditions in all biological systems [12]. Under glycolysis, MGO arises from two intermediates, glyceraldehyde phosphate and dihydroxyacetone phosphate by non-enzymatic phosphate elimination [13, 14]. Moreover, MGO may form through lipid peroxidation and from an intermediate of threonine catabolism, 3-aminoacetone [14]. The MGO within AGE causes irreversible effects on protein structure and function, associated with misfolding [15], and leading to cell apoptosis in various cell types [16]. Moreover, MGO is released upon photodegradation of bisretinoids, A2E and all-*trans*-retinal dimer, which accumulate as lipofuscin in RPE [8]. It can suppress proliferation of RPE cells and enhance autophagy flux [17]. However, the RPE death mechanism related to endoplasmic reticulum (ER) stress that caused by MGO remains elusive.

The ER is a site for protein folding and maturation, as well as an intracellular location for Ca^{2+} store that plays a crucial role in signal transduction [18]. ER stress triggers the unfolded protein response (UPR), which is distinguished by the action of three signalling proteins named inositol-requiring 1 alpha (IRE1α)/spliced X-box binding protein 1 (XBP1), double-strand RNA activated kinase-like ER kinase (PERK)/eukaryotic translation initiation factor 2 alpha (eIF2α)/activating transcription factor 4 (ATF4) and ATF6 [19]. CCAAT/enhancer-binding protein homologous protein (CHOP) (also known as growth arrest and DNA-damage-inducible protein GADD153) is a pro-apoptotic transcription factor associated exclusively with ER stress-induced apoptosis [19]. Many studies showed that ER stress is associated with DR [20, 21] and AMD [22]. MGO has been shown to induce ER stress in lens epithelial cells [23]. However, the link between MGO-induced ER stress and cell death remains unknown. As MGO is highly related to DR and AMD, it is crucial to understand the underlying mechanism of causing RPE cell death. In this study, we found MGO can induce ARPE-19 cell death through an active oxygen species (ROS)-dependent manner, involving mitochondrial membrane potential (MMP) loss, intracellular calcium increase and ER stress response. Moreover, store-operated calcium (SOC) channel inhibitor and ER chaperon can block the MGO-induced ROS production, MMP loss and intracellular calcium increase in ARPE-19 cells.

Materials and methods

Materials

Methylglyoxal, 3-(4,5-dimethylthiazol-2-yl)-2,5-diphenyltetrazolium bromide (MTT), N-acetylcysteine (NAC), 4-phenyl butyric acid (4-PBA), MRS1845, YM-58483, caffeine, dichlorodihydrofluorescein diacetate (H_2DCFDA), dihydroethidium (DHE) and propidium iodide (PI) were obtained from Sigma-Aldrich Co (St Louis, MO, USA). Xestospongin C was purchased from Tocris Bioscience (Bristol, UK). Z-Val-Ala-Asp-fluoromethylketone (z-VAD-FMK), salubrinal and 1,2-bis (2-aminophenoxy)ethane-N,N,N′,N′-tetraacetic acid tetrakis/acetoxymethyl ester (BAPTA/AM) were purchased from Calbiochem (Darmstadt, Germany). The antibodies specific for caspase-3, caspase-9, eIF2α, phospho-eIF2α and poly(ADP-ribose) polymerase 1 (PARP1) were purchased from Cell Signalling Technology (Beverly, MA, USA). The antibodies specific for glucose-regulated protein 78 (GRP78), CHOP, PERK, phospho-PERK and β-actin were purchased from Santa Cruz Biotechnology (Santa Cruz, CA, USA). The antibodies specific for ATF4, ATF6, IRE1β and XBP1 were purchased from Abcam (Cambridge, UK).

Cell cultures

Adult human RPE cell line ARPE19 was purchased from Food Industry Research and Development Institute (Hsinchu, Taiwan). These cells were maintained in Dulbecco's Modified Eagle's Medium/Nutrient Mixture F-12 (DMEM/F12) supplemented with 10% foetal calf serum (GibcoBRL, Invitrogen Life Technologies, Carlsbad, CA, USA), 100 units/ml penicillin and 100 μg/ml streptomycin (Sigma-Aldrich Co.). The cells were cultured in a humidified incubator at 37°C and 5% CO_2. For most of the experiments, cells reaching a 90–95% of confluence were starved and synchronized in serum-free DMEM for 24 h before they were subjected to further analysis.

Measurement of cell viability by MTT assay

Cells (10^4/ml) plated in 96-well plates were incubated with the indicated drugs at 37°C. MTT (5 mg/ml) was added for 45 min, then the culture medium was removed, and the formazan granules generated by live cells were dissolved in 100% DMSO and shaken for 10 min. The optical densities (ODs) at 550 and 630 nm were measured using a microplate reader. The net absorbance (OD550–OD630) indicates the enzymatic activity of mitochondria and implies the cell viability.

Flow cytometric annexin V-FITC/PI assay

The cell surface exposure of phosphatidylserine and the plasma membrane impairment of cells were assessed using annexin V–FITC Apoptosis Detection Kit (Calbiochem). Briefly, suspension of treated/control ARPE-19 cells, containing 5×10^5 cells, was washed with PBS and resuspended in 0.5 ml cold binding buffer. Then, 1.25 μl of annexin V-FITC was added and the cells were incubated in the dark for 15 min at room temperature. Following incubation, the cells were centrifuged at $100 \times g$ for 5 min and the supernatant was removed. The cell pellet was resuspended in 0.5 ml cold binding buffer, and 10 μl of the 30 μg/ml PI solution was added. Cell samples were placed on ice, away from light, and FITC and PI fluorescence was immediately measured by using flow cytometer (Cytomics FC500; Beckman-Coulter, Brea, CA, USA). Data were analysed using CellQuest Pro software (Becton Dickinson, Franklin Lakes, NJ, USA). The populations of live cells, early apoptotic cells, late apoptotic and necrotic cells were determined.

Flow cytometric PI uptake assay

The cell membrane integrity was determined by the ability of cells to take up PI. After trypsinization, cells were collected by centrifugation, washed once with PBS, and resuspended in PBS containing 25 μg/ml PI for 20 min at 37°C. Then, the cells were measured by using flow cytometer (Cytomics FC500; Beckman-Coulter). Data were evaluated using CellQuest Pro software (Becton Dickinson). The level of PI taken up by the cells was measured and represented as the percentage of control.

Determination of the cytosolic ROS

Intracellular ROS production was detected using H_2DCFDA and DHE for H_2O_2 and O_2^- respectively. After drug treatment, ARPE-19 cells were washed with PBS and incubated with 10 μM H_2DCFDA or 5 μM DHE at 37°C for 30 min. Subsequently, the cells were washed in PBS, trypsinized and the fluorescence intensity was measured by flow cytometry (Cytomics FC500; Beckman-Coulter) at excitation/emission wavelengths of 485/530 nm and 488/512 nm for H_2O_2 and O_2^- respectively. For each sample, H_2O_2 or O_2^- production was expressed as mean fluorescence ratio (fluorescence of exposed cells/fluorescence of control cells) from the same experiment.

Determination of the mitochondrial membrane potential (MMP)

Rhodamine 123 is a fluorescent cationic dye that binds to polarized mitochondrial membrane and accumulates as aggregates in the mitochondria of normal cells. ARPE-19 cells were cultured in the absence or presence of MGO for 6 h, and then incubated with 1 μM rhodamine 123 for 30 min. The cells were then centrifuged and resuspended in PBS. Changes in the MMP were detected by flow cytometry (Cytomics FC500; Beckman-Coulter).

Intracellular calcium measurement

Intracellular calcium was measured by Fluo-3. After treating cells with the indicated drugs for different time periods, cells were incubated in PBS containing Fluo-3 (3 μM) for 30 min at 37°C. Cells were subjected to a flow analysis by flow cytometry (Cytomics FC500; Beckman-Coulter).

Cell lysate preparation and Western blot analysis

After stimulation, the medium was aspirated. Cells were rinsed twice with ice-cold PBS, and 25–100 μl of cell lysis buffer (20 mM Tris–HCl, pH 7.5, 125 mM NaCl, 1% Triton X-100, 1 mM $MgCl_2$, 25 mM β-glycerophosphate, 50 mM NaF, 100 μM Na_3VO_4, 1 mM PMSF, 10 μg/ml leupeptin and 10 μg/ml aprotinin) was then added to each well. After harvesting, cell lysates were sonicated and centrifuged, and equal protein amounts of soluble protein, as determined by the Bradford protein assay, were denatured, subjected to sodium dodecylsulfate polyacrylamide gel electrophoresis (SDS-PAGE), and transferred to a polyvinylidene difluoride membrane. Non-specific binding was blocked with TBST (50 mM Tris–HCl, pH 7.5, 150 mM NaCl and 0.02% Tween 20) containing 5% non-fat milk for 1 h at room temperature. After immunoblotting with the first specific antibody, membranes were washed three times with TBST and incubated with a horseradish peroxidase (HRP)-conjugated secondary antibody for 1 h. The dilution folds of first specific antibodies were 1:1000 and β-actin was 1:10,000. After three washes with TBST, the protein bands were detected with enhanced chemiluminescence detection reagent. To make sure equal amounts of sample protein were applied for electrophoresis and immunoblotting, β-actin was used as an internal control.

Statistical analysis

All data were obtained from at least three separate experiments and presented as mean ± standard error (SE). Analysis of variance was used to assess the statistical significance of the differences. A P value of less than 0.05 was considered statistically significant.

Results

Methylglyoxal induces a mixed type of cell death in ARPE-19 cells

To understand the effect of MGO on cell viability, ARPE-19 cells were treated with 100, 300 or 500 μg/ml MGO for 1, 3 and 6 h followed by an annexin V-FITC/PI double labelling assay. The percentages of viable (annexin V-negative/PI-negative), early apoptotic (annexin V-positive/PI-negative), late apoptotic (annexin V-positive/PI-positive) and necrotic cells (annexin V-negative/PI-positive) were determined. Under the 100 μg/ml MGO treatment for 6 h, the cell death is moderate. However, increasing concentration to 300 μg/ml, the percentage of viable cells within 6 h incubation was significantly decreased from 97.3% to 42.4%, the portion of late apoptotic cells was significantly increased from 0.9% to 25.9% and the fraction of necrotic cells was increased from 1.3% to 31.5% at 6 h (Fig. 1A). At higher concentration of MGO (500 μg/ml), there was no viable cells left after 6 h incubation, and the portion of late apoptotic cells was rapidly increased in 1 h incubation, much faster than the onset time (6 h) for 300 μg/ml. The results suggest that MGO at concentrations tested induces an early necrotic cell death, which is followed by the exposure of the apoptotic marker phosphatidylserine. MGO-induced ARPE-19 cells death was further confirmed by the MTT assay after treatment with MGO (10–500 μg/ml) for 2, 6 and 24 h. Data revealed that MGO reduced cell viability in a concentration-dependent manner and the cell viability was reduced by 40% at 300 μg/ml MGO in 6 h (Fig. 1B).

Since caspase activation is one of the mechanisms of apoptotic process, we examined the effect of MGO on caspase activation. ARPE-19 cells were treated with 300 μg/ml MGO and cleavage of caspase-9, -3 and PARP1 were detected by Western blot analysis. The results showed a gradual increase of the cleaved fragments of caspase-9, -3 and PARP1 by MGO treatment for 12 h (Fig. 1C). To

Journal of Cellular and Molecular Medicine published by John Wiley & Sons Ltd and Foundation for Cellular and Molecular Medicine.

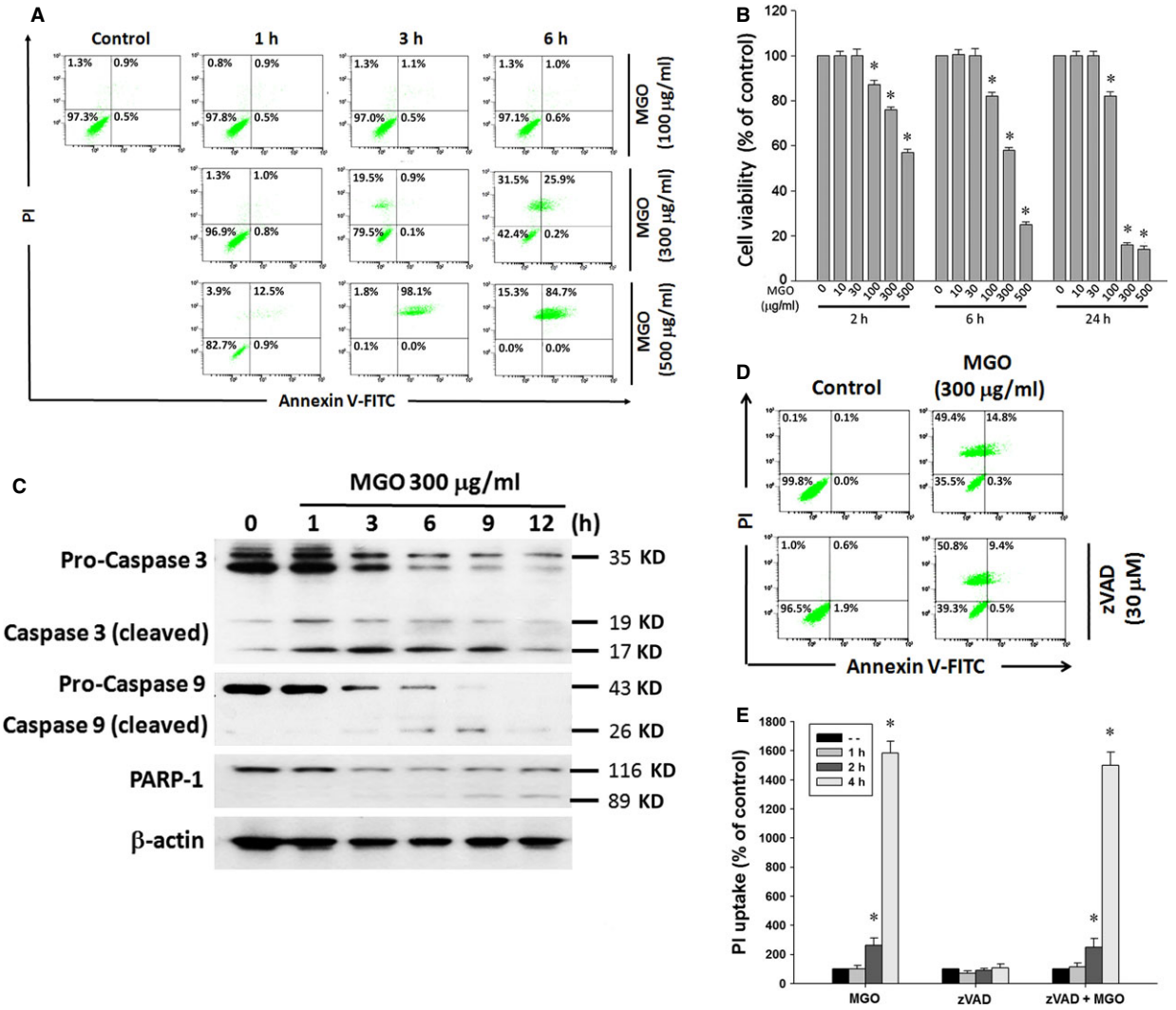

Fig. 1 MGO decreases cell viability and induces caspase-independent cell death in ARPE-19 cells. (**A**) Cells were treated with various concentrations (100, 300 or 500 μg/ml) of MGO for 1, 3 or 6 h, and then stained with annexin V and PI, and evaluated by flow cytometry. (**B**) Cells were treated with various concentrations (10–500 μg/ml) of MGO for 2, 6 or 24 h. Cell viability was determined by MTT assay and the percentages of viability as compared to vehicle-treated cells were plotted as the mean ± SE of at least three independent experiments. (**C**) Cells were treated with 300 μg/ml MGO for the indicated times. Cells were lysed and expression levels of indicated proteins were detected by Western blotting by using antibodies against caspase 3, caspase 9, PARP-1 and β-actin. (**D**) Cells were treated with pan-caspase inhibitor zVAD (30 μM) for 30 min, followed by the treatment with 300 μg/ml MGO for 6 h. Cell viability was determined by annexin V/PI double staining assay. (**E**) After cells were treated with zVAD and MGO (300 μg/ml) for 1, 2 and 4 h, PI uptake was measured by flow cytometry. $*P < 0.05$, indicating the significant induction of cell death by MGO.

determine whether caspase is a crucial factor in MGO-induced apoptosis in ARPE-19 cells, cells were pre-treated with pan-caspase inhibitor zVAD for 1 h, followed by treatment with 300 μg/ml MGO for 6 h. Cell viability by annexin V-FITC/PI double labelling assay showed that viable cells were significantly decreased at 6 h, but this portion of viable cells cannot be reversed by adding zVAD (Fig. 1D), indicating MGO induces a caspase-independent mixed type of cell death. Consistently, data of PI uptake revealed that MGO-induced cell necrosis was not altered by zVAD (Fig. 1E).

Increased mitochondrial ROS production contributes to mitochondrial membrane potential loss and cell death caused by MGO

To determine whether MGO could induce accumulation of ROS in ARPE-19 cells, cells were treated with 300 μg/ml MGO for the indicated time within 1 h, and were then treated with H_2DCFDA or DHE for 30 min. The data of flow cytometry indicated that

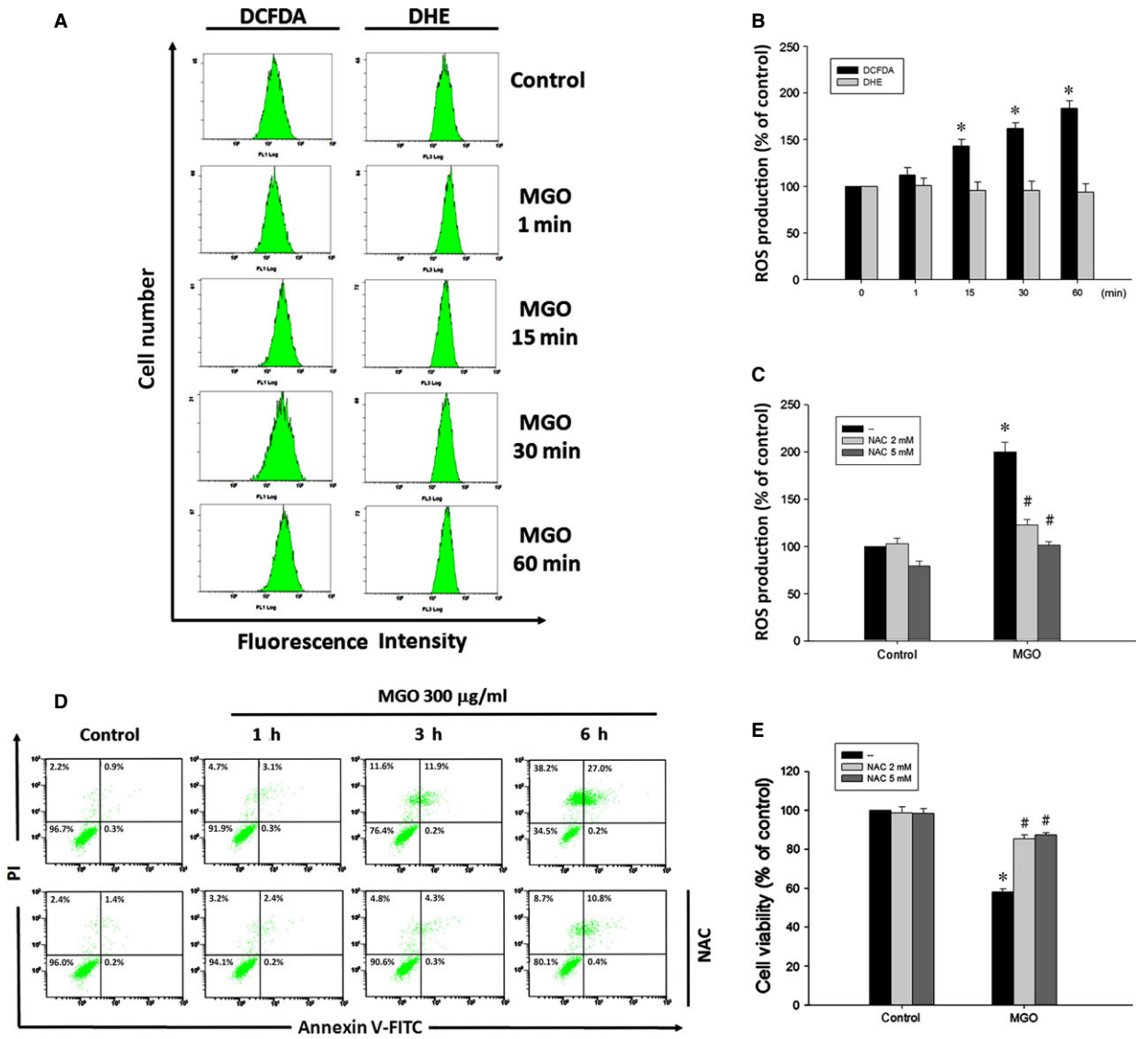

Fig. 2 ROS scavenger suppresses MGO-induced ROS generation and cell death in ARPE-19 cells. (**A, B**) Cells were incubated with 300 μg/ml MGO for the indicated times, and then treated with H_2DCFDA (10 μM) or DHE (5 μM) for 30 min. Cellular ROS levels were measured using flow cytometry, and presented as percentages of control. (**C**) After pre-treatment with 2 or 5 mM NAC for 30 min, MGO-induced mitochondrial ROS production at 1 h was measured with H_2DCFDA by using flow cytometry. (**D**) MGO-induced cell death was assessed by pre-treatment with NAC (2 mM) for 6 h. Cells were stained with annexin V and PI, and evaluated by flow cytometry. (**E**) Cell viability was determined by MTT assay at 6 h. $^*P < 0.05$, indicating the significant increase of mitochondrial ROS production (**B, C**) and decrease of cell viability (**E**) by MGO. $^{\#}P < 0.05$, indicating the significant effects of NAC to reverse the actions of MGO in ROS production (**C**) and cell death (**E**).

H_2O_2 generation was rapidly increased by MGO at 15 min (47.5%) and kept increasing to 96.7% at 1 h. However, cellular O_2^- was not increased (Fig. 2A and B). Pre-treatment with 2 or 5 mM NAC abrogated MGO-induced ROS production at 1 h (Fig. 2C). Concomitantly, NAC can reverse the MGO-induced cell death as indexed by both the annexin V-FITC/PI double labelling (Fig. 2D) and MTT assay (Fig. 2E). These results suggest the involvement of mitochondrial ROS in MGO-induced cell death in ARPE-19 cells.

Since mitochondrial integrity is highly related to the cell viability, we determined whether MGO induces mitochondrial dysfunction by testing the MMP of the RPE cells. Cells were treated with 300 μg/ml MGO for the indicated time within 4 h, and the MMP was measured with rhodamine 123 by using flow cytometry. Results revealed the

Journal of Cellular and Molecular Medicine published by John Wiley & Sons Ltd and Foundation for Cellular and Molecular Medicine.

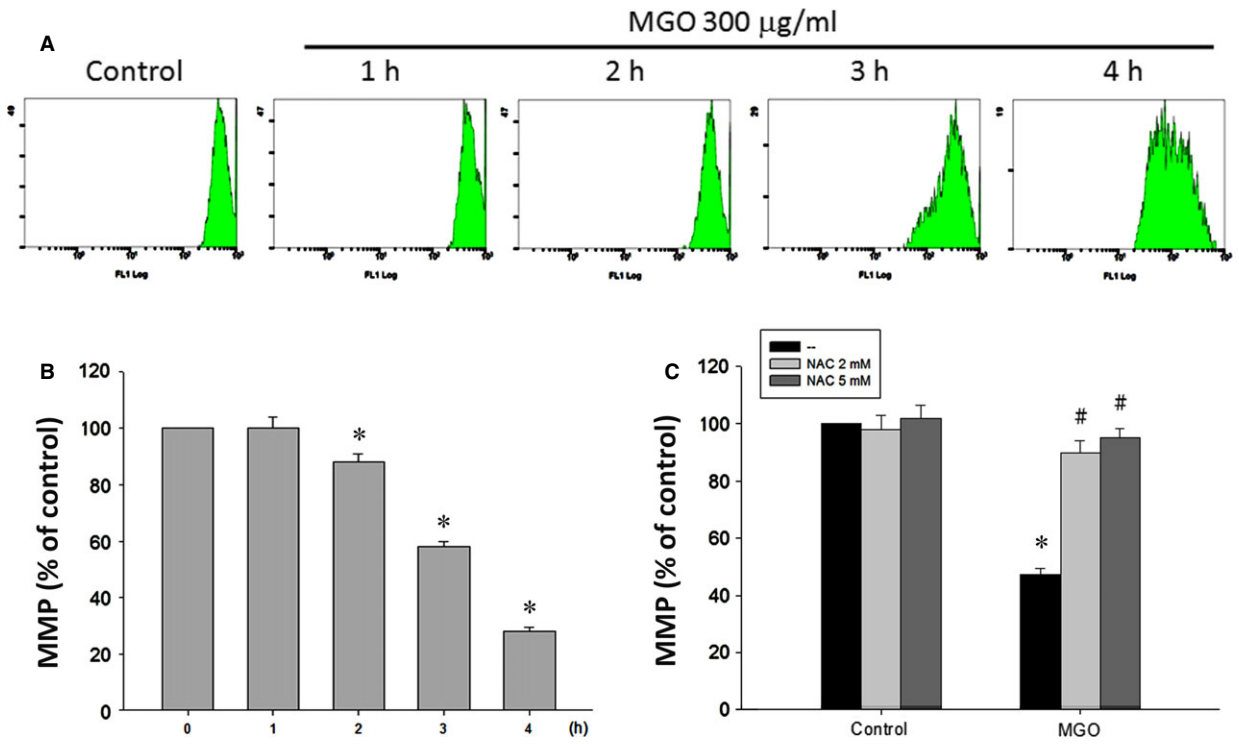

Fig. 3 ROS scavenger suppresses MGO-induced MMP reduction in ARPE-19 cells. (**A, B**) Cells were incubated with 300 μg/ml MGO for 1, 2, 3 or 4 h. MMP was measured with rhodamine 123 by using flow cytometry. (**C**) Cells were pre-incubated with 2 or 5 mM NAC for 30 min and then incubated with 300 μg/ml MGO for 3 h. $^{*}P < 0.05$, indicating the significant decrease of MMP by MGO. $^{\#}P < 0.05$, indicating the significant ability of NAC to restore MMP under MGO treatment.

MMP loss from 1 to 4 h progressively (Fig. 3A and B), and this event was completely reversed by NAC (Fig. 3C). These results suggest that increased ROS contributes to the loss of MMP under MGO treatment in RPE cells.

MGO increases intracellular calcium level through SOC pathway, and intracellular calcium and ROS exert an amplified effect to induce MMP loss

As calcium is a critical signal in the cell death pathway, we tested whether cytosolic calcium level is changed after MGO treatment. As a result, MGO can increase the intracellular calcium level in RPE cells after 1 h of incubation, and this increasing effect continued to 6 h by 6.3 folds (Fig. 4A and B). In order to understand the sources and pathway for intracellular calcium elevation, we examined the MGO-induced intracellular calcium levels with the use of the SOC channel inhibitors, MRS1845 and YM-58483 [24–26], as well as the selective and membrane permeable IP_3 receptor inhibitor xestospongin C [27, 28]. We found that MRS1845 and YM-58483 can significantly block the increase of the intracellular calcium, while xestospongin C did not have this effect (Fig. 4C). Moreover, caffeine, a ryanodine receptor activator [29] also failed to affect the increased intracellular calcium (Fig. 4C). These results suggest that MGO can induce extracellular calcium entry through SOC pathway.

Afterwards, we examined the mutual interaction of the increased intracellular calcium and ROS under MGO stimulation. We found that NAC (2 and 5 mM) can reverse the MGO-induced intracellular calcium increase in a concentration-dependent manner (Fig. 5A). Conversely, calcium chelator BAPTA/AM and SOC channel inhibitors, MRS1845 and YM-58483, can inhibit MGO-induced ROS production at 1 h (Fig. 5B). In contrast, IP_3 receptor inhibitor xestospongin C and aryanodine receptor activator caffeine cannot affect intracellular calcium increase caused by MGO (Fig. 5B). Consistently, MRS1845 and YM-58483, but not xestospongin C and caffeine, can reverse the MGO-induced MMP loss (Fig. 5C). These results altogether suggest the existence of an amplification effect of mitochondrial ROS production and SOC-mediated calcium influx, and the coordinated effect to decrease MMP under MGO treatment.

MGO-induced ER stress response mediates ROS production, calcium increase and MMP loss

As MGO can induce ER stress in lens epithelial cells [23], we determined whether MGO could also induce ER stress in RPE cells. First, we found the time-dependent effects of MGO within 6 h to increase

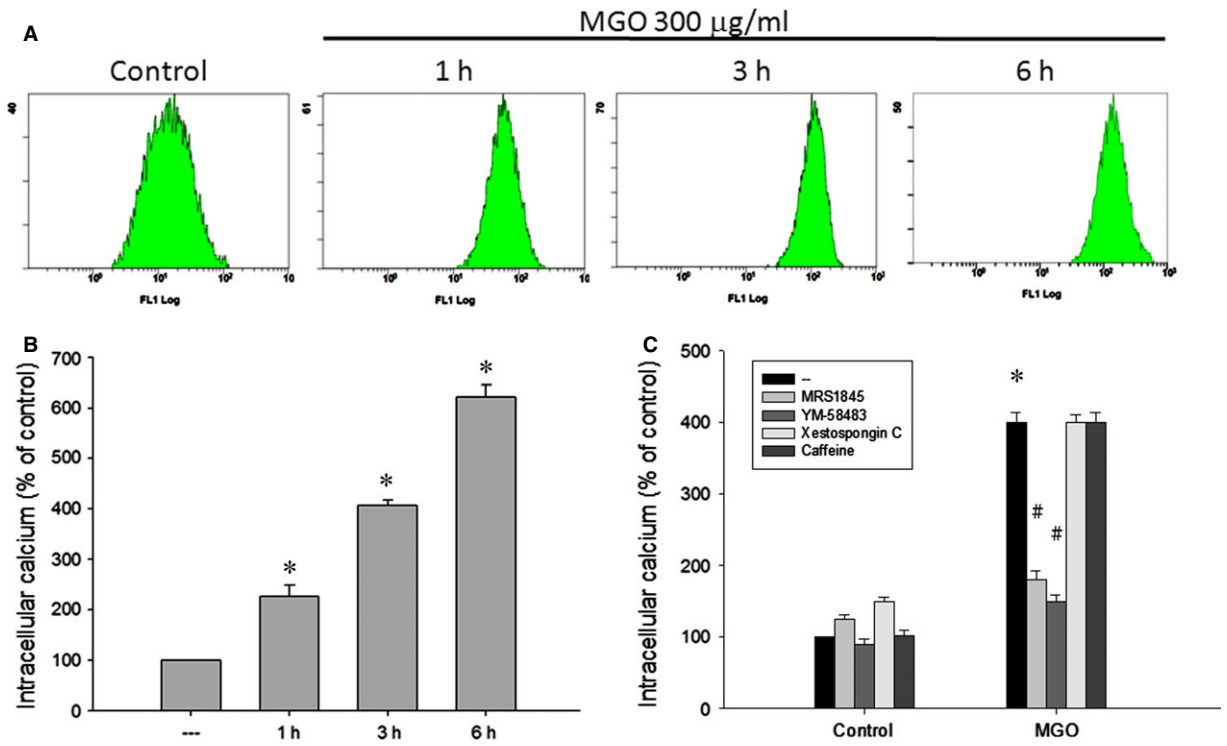

Fig. 4 SOC channel inhibitors reduce MGO-induced intracellular calcium increase in ARPE-19 cells. (**A, B**) Cells were incubated with 300 μg/ml MGO for 1, 3 or 6 h. (**C**) Cells were pre-treated with MRS1845 (10 μM), YM-58483 (10 μM), xestospongin C (1 μM) or caffeine (10 mM) for 30 min, and then incubated with 300 μg/ml MGO for 3 h. Intracellular calcium levels were determined by using Fluo-3 AM and flow cytometry. $^{*}P < 0.05$, indicating the significant increase of intracellular calcium level by MGO. $^{\#}P < 0.05$, indicating the significant inhibition of MGO-elicited intracellular calcium increase.

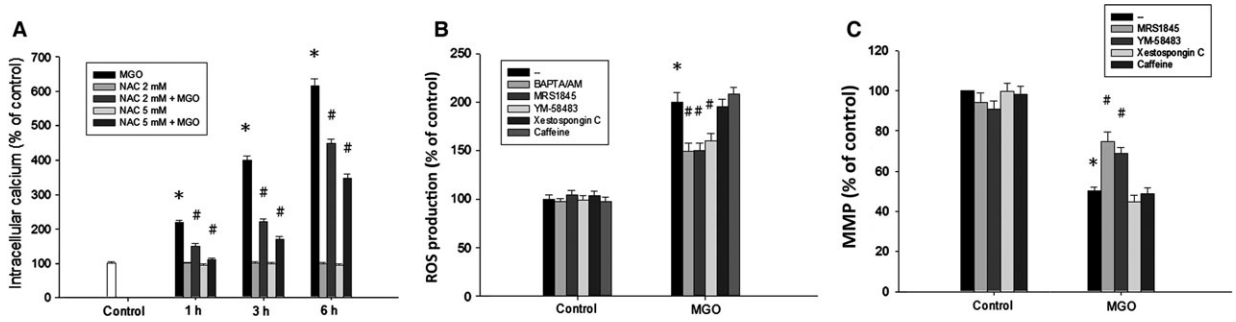

Fig. 5 Reciprocal amplification of ROS production and intracellular calcium increase in MGO-treated ARPE-19 cells. (**A**) Cells were pre-incubated with NAC (2 or 5 mM) for 30 min and then incubated with 300 μg/ml MGO for 1, 3 or 6 h. Intracellular calcium levels were determined by using Fluo-3 AM and flow cytometry. (**B, C**) Cells were pre-treated with BAPTA/AM (10 μM), MRS1845 (10 μM), YM-58483 (10 μM), xestospongin C (1 μM) or caffeine (10 mM) for 30 min and then incubated with 300 μg/ml MGO. After 1 h, cellular ROS levels were measured with H_2DCFDA by using flow cytometry (**B**). After 3 h, MMP was measured with rhodamine 123 by using flow cytometry (**C**). $^{*}P < 0.05$, indicating the significant effects of MGO. $^{\#}P < 0.05$, indicating the significant inhibition of MGO responses by indicated agents.

the protein expressions of GRP78, CHOP, ATF6 and ATF4, protein phosphorylation of eIF2α and PERK, and spliced XBP1and ATF6 formation (Fig. 6). These data suggest the ability of MGO to induce ER stress response.

To elucidate the role of ER stress in MGO-induced cell death, we used chemical inhibitors of ER stress, i.e. salubrinal, a selective inhibitor of eIF2α dephosphorylation [30], and 4-PBA, a chemical chaperone of ER [31]. When ARPE-19 cells were pre-treated with 10 μM

Journal of Cellular and Molecular Medicine published by John Wiley & Sons Ltd and Foundation for Cellular and Molecular Medicine.

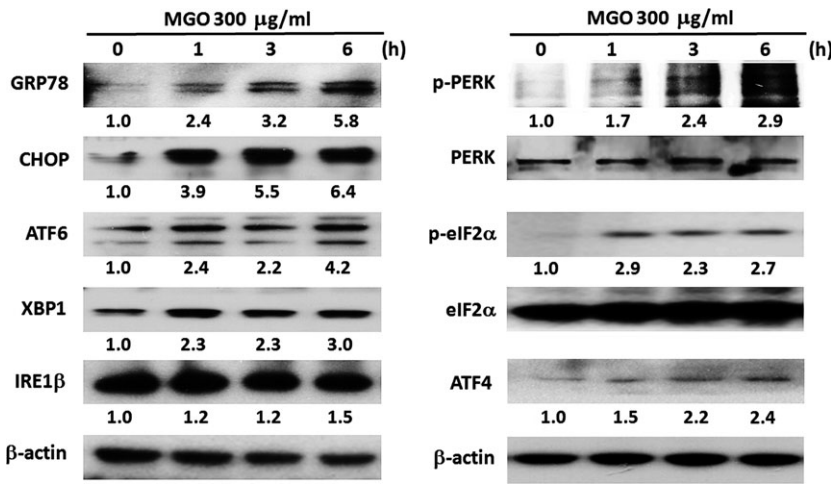

Fig. 6 MGO induces ER stress response in ARPE-19 cells. Cells were treated with 300 μg/ml MGO for the indicated times. Cell lysates were analysed by Western blot with antibodies specific to GRP78, CHOP, ATF6α (p90), XBP1, IRE1β, p-PERK, PERK, p-eIF2α, eIF2α, ATF4 and β-actin. Results were representative of three independent experiments. The changes of protein expression were normalized to β-actin (the cases of GRP78, CHOP, ATF6, XBP-1, IRE1β and ATF4) or total protein (the cases for PERK and eIF2α), and then compared to the control group without MGO treatment.

salubrinal or 3 mM 4-PBA for 1 h and then incubated with MGO for 1 h, the MGO-induced ROS generation (Fig. 7A and B) as well as MMP loss (Fig. 7C) was significantly decreased. Likewise, both ER stress inhibitors can reduce the MGO-induced intracellular calcium increase (Fig. 7D). Accordingly, salubrinal (10 μM) significantly reversed MGO-induced cell death in ARPE-19 cells (Fig. 7E). The viable cells were significantly increased from 38.4% to 75.9% by salubrinal. The results suggest that ER stress plays a key role in MGO-induced ROS-dependent cell death.

Discussion

MGO is a physiological metabolite that is closely related to the pathogenesis in AMD and DR. Chronic hyperglycaemia induces elevated levels of intracellular production of MGO [32], and MGO may be the major source of AGEs in retina [33]. Moreover, MGO is important in mediating microglial activation in the diabetic retina [34]. As a highly reactive dicarbonyl metabolite, MGO can alter molecular structure and function by forming AGE-adducts with proteins, phospholipids and nucleotides. For AGEs containing MGO, they can damage cells by three general mechanisms: as adducts occurring on modified serum proteins, as endogenous adducts formed as a consequence of glucose metabolism, or as extracellular matrix-immobilized modifications on long-lived structural proteins [7]. MGO also plays an important role in the formation of drusen, which accumulates below RPE cells and is related to the AMD. Under the vitamin A cycling in retina, fluorescent bisretinoids, such as A2E and all-*trans*-retinal dimer, are formed as a by-product and can accumulate in RPE cells as lipofuscin pigments. Further photo-cleavage of A2E can produce reactive dicarbonyl MGO [35]. Moreover, in the pathogenesis of AMD, the collagen of Bruch's membrane is increasingly cross-linked with age [36], and MGO is a critical contributor to this covalent cross-linking of extracellular proteins [8]. Previously, MGO at the mM concentration range has been shown to affect various kinds of cellular functions such as insulin signalling [37], mitochondrial respiration and glycolysis [38]. Moreover, high dose MGO therapy has been suggested for the cancer treatment [39–41]. But its side effects on the normal tissue should be taken into consideration.

Apoptosis is an active physiological process to self-destruction for maintaining cellular homeostasis between cell division and cell death. MGO has been demonstrated to induce apoptosis in several cell types [42–44], including RPE cell [45]. Our study also showed that MGO decreases cell viability and induces a mixed type of cell death in ARPE-19 cells (Fig. 1A and B). After MGO (300 μg/ml) treatment, early necrosis followed by appearance of phosphatidylserine is

Fig. 7 ER stress inhibitors suppress MGO-induced ROS generation, MMP reduction, intracellular calcium increase and cell death in ARPE-19 cells. Cells were pre-treated with 10 μM salubrinal or 3 mM 4-phenylbutyrate (PBA) for 1 h and then incubated with 300 μg/ml MGO. (**A, B**) After MGO incubation for 1 h, cellular ROS levels were measured with H_2DCFDA by using flow cytometry. (**C**) After MGO incubation for 3 h, MMP was measured with rhodamine 123 by using flow cytometry. (**D**) After MGO incubation for 3 h, intracellular calcium levels were determined by using Fluo-3 AM and flow cytometry. $^*P < 0.05$, indicating the significant effect of MGO alone. $^{\#}P < 0.05$, indicating the significant inhibitory effects of salubrinal and PBA on MGO responses. (**E**) After MGO incubation for 6 h, cell viability was determined by annexin V and PI staining, and evaluated by flow cytometry.

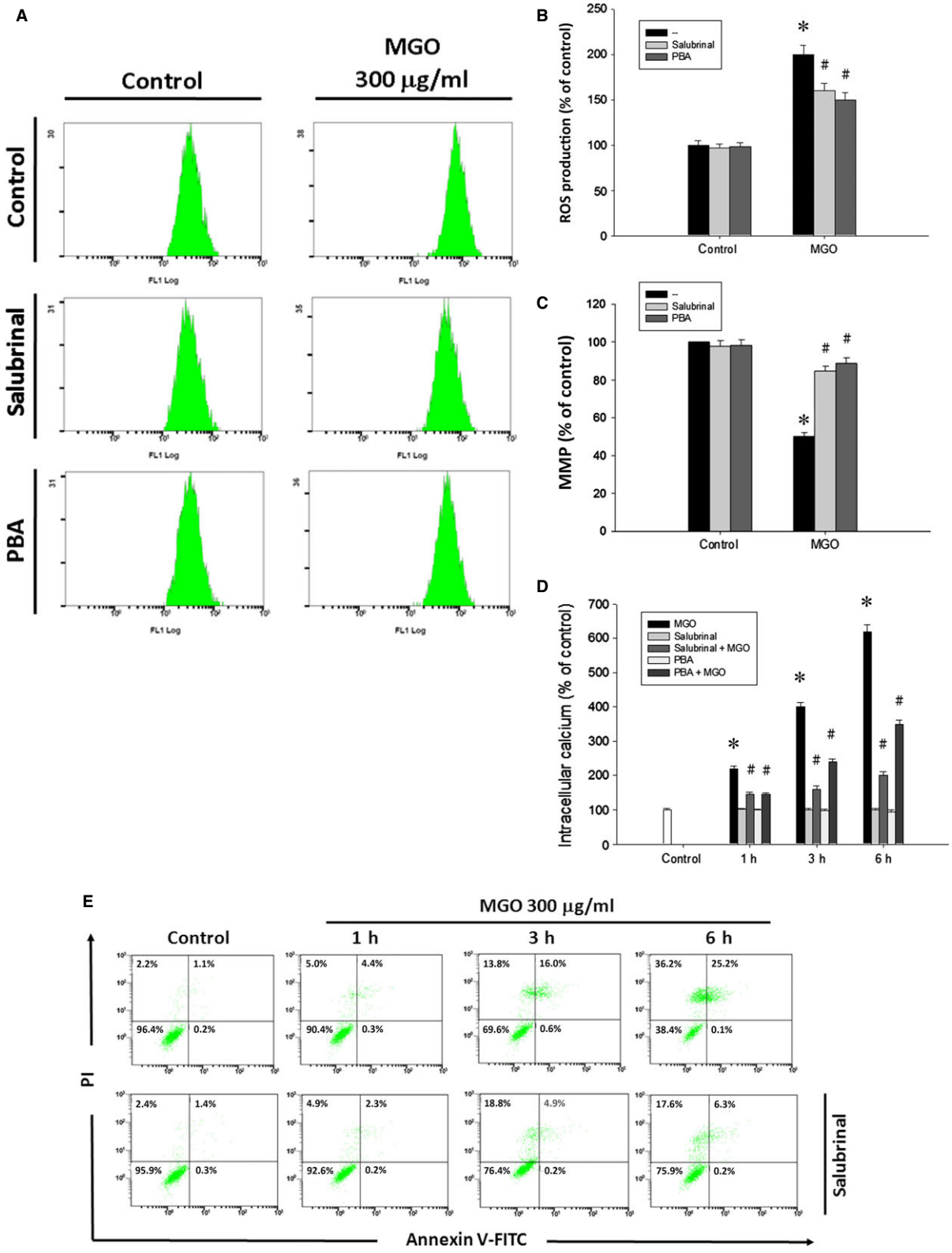

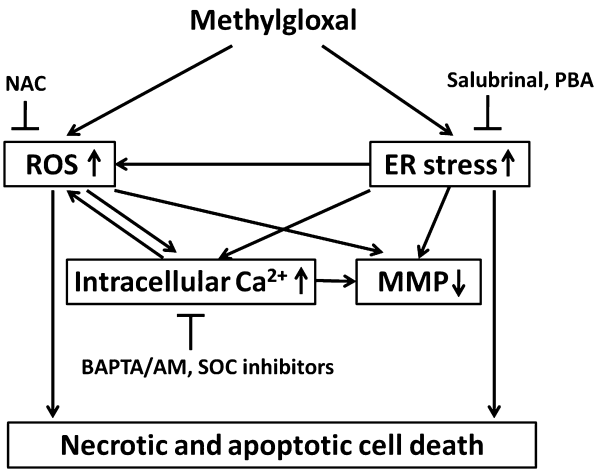

Fig. 8 Summary of molecular mechanisms underlying MGO-induced cell death in RPE cells.

a unique feature, because in most examples of cell death, early apoptosis can lead to late necrosis. We currently do not have any explanations for such feature of cell death. As caspase activation is an important process in apoptosis, we showed a gradual increase of the cleaved fragments of caspase-9, -3 and PARP1 by MGO treatment within 3–12 h (Fig. 1C). However, pan-caspase inhibitor zVAD cannot reverse the cell death process (Fig. 1D and E). Therefore, we suggest that MGO-induced cell death is independent of caspase activity; the exposure of late apoptosis marker and caspase activation are consequences of cell necrosis.

MGO has been shown to induce oxidative stress in osteoblast [44] and endothelial cells [46]. Our study showed that MGO-induced RPE cell death is through the oxidative stress coming from H_2O_2 rather than O_2^- (Fig. 2A and B). Oxidative stress has been studied extensively in relation to the pathophysiology of AMD and is suggested to have a crucial role [47]. As the location and physiological function of RPE cells, they are constantly exposed to several ROS [48]. Thus, the protection of RPE cells by the antioxidants from oxidative damage is an important consideration for treating AMD. In this study, treatment with antioxidants resulted in much lower levels of MGO-induced intracellular production of ROS. Moreover, our results from flow cytometry showed that MGO-induced cell death in ARPE-19 cells is greatly reduced by treatment with antioxidants (Fig. 2C–E). MGO may reduce viability *via* alterations in mitochondrial integrity [43, 44, 49]. Mitochondrial integrity is crucial for cell survival, and decreased MMP is an early sign of apoptosis. Our results demonstrated that RPE cells have mitochondrial dysfunction when exposed to MGO. At higher ROS levels, longer mitochondrial permeability transition pore openings may release a ROS burst leading to destruction of mitochondria, and the released ROS can further propagate from one mitochondrion to another mitochondrion in a cell [50]. Therefore, the decline in MMP caused by MGO (Fig. 3A and B) could be prevented by treating antioxidant NAC (Fig. 3C).

Elevated intracellular Ca^{2+} concentration initiates apoptosis in many cell types. Our study showed that MGO treatment causes an increase in cytoplasmic Ca^{2+} (Fig. 4A and B). SOCs are the plasma membrane Ca^{2+} channels which are a major pathway for Ca^{2+} entry under the condition of decreased Ca^{2+} content in the ER [51]. Our study shows the SOC channel inhibitor can completely block the increase of the intracellular calcium (Fig. 4C). IP_3 receptors are ligand-gated channels that discharge Ca^{2+} from ER stores in response to stimuli [52]. The release of Ca^{2+} from ER stores by IP_3 receptors induces mitochondrial Ca^{2+} overload and cell death [53]. Our results demonstrate that the IP_3 receptor inhibitor cannot lower the increased intracellular calcium by MGO (Fig. 4C). According to some reports, ROS can induce an increase in intracellular Ca^{2+} concentration [54, 55], and calcium released from the ER augments the production of cytosolic ROS [56]. In the present study, our data also support this notion. The increased intracellular Ca^{2+} by MGO could be reversed by antioxidant NAC (Fig. 5A). Besides, lowering intracellular Ca^{2+} by intracellular calcium chelator BAPTA/AM and SOC channel inhibitors can reduce the MGO-induced ROS generation (Fig. 5B). Furthermore, decreasing intracellular Ca^{2+} by SOC channel inhibitors can reduce the MGO-induced MMP loss (Fig. 5C).

ER stress plays a major pathological role in many ocular diseases such as retinitis pigmentosa, glaucoma and macular degeneration [57]. Induction of stress by MGO in human lens epithelial cells has been demonstrated [23], but ER stress-induced cell death by MGO in RPE cells is not known. Our studies indicate that MGO activates the initiators of typical UPR signal transduction pathways: PERK-eIF2α-ATF4, IRE1-XBP1 and ATF6 (Fig. 6). In order to confirm the role of ER stress in MGO-induced cell death, we used two different chemical ER stress inhibitors, salubrinal and 4-PBA. The pre-treatment with salubrinal or 4-PBA can decrease the MGO-induced ROS generation (Fig. 7A and B) and intracellular calcium elevation (Fig. 7D), and can reverse the MMP loss and cell death by MGO (Fig. 7C and E). These results altogether suggest that ER stress plays a key role in MGO-induced cell death.

In conclusion, we, for the first time, demonstrate that MGO can decrease RPE cell viability, resulting from the ER stress-dependent intracellular ROS production, MMP loss and increased intracellular calcium (Fig. 8). ROS scavenger and store-operated calcium channel inhibitors can reverse the MGO-induced ROS production, MMP loss, intracellular calcium increase and cell death. Besides, inhibition of ER stress by salubrinal and 4-PBA can reduce the MGO-induced intracellular events and cell death. As MGO is one of the components of drusen in AMD and is the AGEs adduct in DR, this study could provide a valuable insight into the molecular pathogenesis of AMD and DR.

Acknowledgement

This research work was supported by MOST 103-2320-B-038-025 -MY3, 102CGH-TMU-01-1, 103CGH-TMU-01-1, CTH-102-1-2A30 and CTH-103-27.

Conflict of interest

The authors declare that they have no conflict of interest.

References

1. **Simo R, Villarroel M, Corraliza L, *et al.*** The retinal pigment epithelium: something more than a constituent of the blood-retinal barrier–implications for the pathogenesis of diabetic retinopathy. *J Biomed Biotechnol*. 2010; 2010: 190724.
2. **Bhutto I, Lutty G.** Understanding age-related macular degeneration (AMD): relationships between the photoreceptor/retinal pigment epithelium/Bruch's membrane/choriocapillaris complex. *Mol Aspects Med*. 2012; 33: 295–317.
3. **Saaddine JB, Honeycutt AA, Narayan KM, *et al.*** Projection of diabetic retinopathy and other major eye diseases among people with diabetes mellitus: United States, 2005-2050. *Arch Ophthalmol*. 2008; 126: 1740–7.
4. **Congdon N, O'Colmain B, Klaver CC, *et al.*** Causes and prevalence of visual impairment among adults in the United States. *Arch Ophthalmol*. 2004; 122: 477–85.
5. **Mettu PS, Wielgus AR, Ong SS, *et al.*** Retinal pigment epithelium response to oxidant injury in the pathogenesis of early age-related macular degeneration. *Mol Aspects Med*. 2012; 33: 376–98.
6. **Glenn JV, Stitt AW.** The role of advanced glycation end products in retinal ageing and disease. *Biochim Biophys Acta*. 2009; 1790: 1109–16.
7. **Stitt AW.** AGEs and diabetic retinopathy. *Invest Ophthalmol Vis Sci*. 2010; 51: 4867–74.
8. **Yoon KD, Yamamoto K, Ueda K, *et al.*** A novel source of methylglyoxal and glyoxal in retina: implications for age-related macular degeneration. *PLoS ONE*. 2012; 7: e41309.
9. **Glenn JV, Beattie JR, Barrett L, *et al.*** Confocal Raman microscopy can quantify advanced glycation end product (AGE) modifications in Bruch's membrane leading to accurate, nondestructive prediction of ocular aging. *FASEB J*. 2007; 21: 3542–52.
10. **Zong H, Ward M, Stitt AW.** AGEs, RAGE, and diabetic retinopathy. *Curr Diab Rep*. 2011; 11: 244–52.
11. **Yamada Y, Ishibashi K, Ishibashi K, *et al.*** The expression of advanced glycation end-product receptors in rpe cells associated with basal deposits in human maculas. *Exp Eye Res*. 2006; 82: 840–8.
12. **Kalapos MP.** Where does plasma methylglyoxal originate from? *Diabetes Res Clin Pract*. 2013; 99: 260–71.
13. **Allaman I, Belanger M, Magistretti PJ.** Methylglyoxal, the dark side of glycolysis. *Front Neurosci*. 2015; 9: 23.
14. **Maessen DE, Stehouwer CD, Schalkwijk CG.** The role of methylglyoxal and the glyoxalase system in diabetes and other age-related diseases. *Clin Sci (Lond)*. 2015; 128: 839–61.
15. **Sousa Silva M, Gomes RA, Ferreira AE, *et al.*** The glyoxalase pathway: the first hundred years. . . and beyond. *Biochem J*. 2013; 453: 1–15.
16. **Di Loreto S, Zimmitti V, Sebastiani P, *et al.*** Methylglyoxal causes strong weakening of detoxifying capacity and apoptotic cell death in rat hippocampal neurons. *Int J Biochem Cell Biol*. 2008; 40: 245–57.
17. **Chang YC, Hsieh MC, Wu HJ, *et al.*** Methylglyoxal, a reactive glucose metabolite, enhances autophagy flux and suppresses proliferation of human retinal pigment epithelial ARPE-19 cells. *Toxicol In Vitro*. 2015; 29: 1358–68.
18. **Krebs J, Agellon LB, Michalak M.** Ca(2+) homeostasis and endoplasmic reticulum (ER) stress: an integrated view of calcium signaling. *Biochem Biophys Res Commun*. 2015; 460: 114–21.
19. **Sano R, Reed JC.** ER stress-induced cell death mechanisms. *Biochim Biophys Acta*. 2013; 1833: 3460–70.
20. **Zhang SX, Ma JH, Bhatta M, *et al.*** The unfolded protein response in retinal vascular diseases: implications and therapeutic potential beyond protein folding. *Prog Retin Eye Res*. 2015; 45: 111–31.
21. **Ma JH, Wang JJ, Zhang SX.** The unfolded protein response and diabetic retinopathy. *J Diabetes Res*. 2014; 2014: 160140.
22. **Zhang SX, Sanders E, Fliesler SJ, *et al.*** Endoplasmic reticulum stress and the unfolded protein responses in retinal degeneration. *Exp Eye Res*. 2014; 125: 30–40.
23. **Palsamy P, Bidasee KR, Ayaki M, *et al.*** Methylglyoxal induces endoplasmic reticulum stress and DNA demethylation in the Keap1 promoter of human lens epithelial cells and age-related cataracts. *Free Radic Biol Med*. 2014; 72: 134–48.
24. **Harper JL, Camerini-Otero CS, Li AH, *et al.*** Dihydropyridines as inhibitors of capacitative calcium entry in leukemic HL-60 cells. *Biochem Pharmacol*. 2003; 65: 329–38.
25. **Ishikawa J, Ohga K, Yoshino T, *et al.*** A pyrazole derivative, YM-58483, potently inhibits store-operated sustained Ca2 + influx and IL-2 production in T lymphocytes. *J Immunol*. 2003; 170: 4441–9.
26. **Gao XH, Gao R, Tian YZ, *et al.*** A store-operated calcium channel inhibitor attenuates collagen-induced arthritis. *Br J Pharmacol*. 2015; 172: 2991–3002.
27. **Vassilev PM, Peng JB, Johnson J, *et al.*** Inhibition of CaT1 channel activity by a non-competitive IP3 antagonist. *Biochem Biophys Res Commun*. 2001; 280: 145–50.
28. **Oka T, Sato K, Hori M, *et al.*** Xestospongin C, a novel blocker of IP3 receptor, attenuates the increase in cytosolic calcium level and degranulation that is induced by antigen in RBL-2H3 mast cells. *Br J Pharmacol*. 2002; 135: 1959–66.
29. **Croisier H, Tan X, Chen J, *et al.*** Ryanodine receptor sensitization results in abnormal calcium signaling in airway smooth muscle cells. *Am J Respir Cell Mol Biol*. 2015; 53: 703–11.
30. **Boyce M, Bryant KF, Jousse C, *et al.*** A selective inhibitor of eIF2alpha dephosphorylation protects cells from ER stress. *Science*. 2005; 307: 935–9.
31. **Cohen FE, Kelly JW.** Therapeutic approaches to protein-misfolding diseases. *Nature*. 2003; 426: 905–9.
32. **Brownlee M.** Biochemistry and molecular cell biology of diabetic complications. *Nature*. 2001; 414: 813–20.
33. **Karachalias N, Babaei-Jadidi R, Ahmed N, *et al.*** Accumulation of fructosyl-lysine and advanced glycation end products in the kidney, retina and peripheral nerve of streptozotocin-induced diabetic rats. *Biochem Soc Trans*. 2003; 31: 1423–5.
34. **Wang J, Lin J, Schlotterer A, *et al.*** CD74 indicates microglial activation in experimental diabetic retinopathy and exogenous methylglyoxal mimics the response in normoglycemic retina. *Acta Diabetol*. 2014; 51: 813–21.
35. **Wu Y, Yanase E, Feng X, *et al.*** Structural characterization of bisretinoid A2E photocleavage products and implications for age-related macular degeneration. *Proc Natl Acad Sci U S A*. 2010; 107: 7275–80.
36. **Booij JC, Baas DC, Beisekeeva J, *et al.*** The dynamic nature of Bruch's membrane. *Prog Retin Eye Res*. 2010; 29: 1–18.
37. **Riboulet-Chavey A, Pierron A, Durand I, *et al.*** Methylglyoxal impairs the insulin signaling pathways independently of the formation of intracellular reactive oxygen species. *Diabetes*. 2006; 55: 1289–99.
38. **Biswas S, Ray M, Misra S, *et al.*** Selective inhibition of mitochondrial respiration and glycolysis in human leukaemic leucocytes by methylglyoxal. *Biochem J*. 1997; 323(Pt 2): 343–8.

Journal of Cellular and Molecular Medicine published by John Wiley & Sons Ltd and Foundation for Cellular and Molecular Medicine.

39. **Milanesa DM, Choudhury MS, Mallouh C, *et al.*** Methylglyoxal-induced apoptosis in human prostate carcinoma: potential modality for prostate cancer treatment. *Eur Urol*. 2000; 37: 728–34.
40. **Antognelli C, Mezzasoma L, Fettucciari K, *et al.*** A novel mechanism of methylglyoxal cytotoxicity in prostate cancer cells. *Int J Biochem Cell Biol*. 2013; 45: 836–44.
41. **Ganapathy-Kanniappan S, Geschwind JF.** Tumor glycolysis as a target for cancer therapy: progress and prospects. *Mol Cancer*. 2013; 12: 152.
42. **Tajes M, Eraso-Pichot A, Rubio-Moscardo F, *et al.*** Methylglyoxal reduces mitochondrial potential and activates Bax and caspase-3 in neurons: implications for Alzheimer's disease. *Neurosci Lett*. 2014; 580: 78–82.
43. **Seo K, Ki SH, Shin SM.** Methylglyoxal induces mitochondrial dysfunction and cell death in liver. *Toxicol Res*. 2014; 30: 193–8.
44. **Suh KS, Choi EM, Rhee SY, *et al.*** Methylglyoxal induces oxidative stress and mitochondrial dysfunction in osteoblastic MC3T3-E1 cells. *Free Radic Res*. 2014; 48: 206–17.
45. **Sook Kim Y, Soo Lee I, Sook Kim J.** Protective effects of puerariae radix extract and its single compounds on methylglyoxal-induced apoptosis in human retinal pigment epithelial cells. *J Ethnopharmacol* 2014; 152: 594–8.
46. **Miyazawa N, Abe M, Souma T, *et al.*** Methylglyoxal augments intracellular oxidative stress in human aortic endothelial cells. *Free Radic Res*. 2010; 44: 101–7.
47. **Jarrett SG, Boulton ME.** Consequences of oxidative stress in age-related macular degeneration. *Mol Aspects Med*. 2012; 33: 399–417.
48. **Plafker SM, O'Mealey GB, Szweda LI.** Mechanisms for countering oxidative stress and damage in retinal pigment epithelium. *Int Rev Cell Mol Biol*. 2012; 298: 135–77.
49. **Wang H, Liu J, Wu L.** Methylglyoxal-induced mitochondrial dysfunction in vascular smooth muscle cells. *Biochem Pharmacol*. 2009; 77: 1709–16.
50. **Zorov DB, Juhaszova M, Sollott SJ.** Mitochondrial reactive oxygen species (ROS) and ROS-induced ROS release. *Physiol Rev*. 2014; 94: 909–50.
51. **Hogan PG, Rao A.** Store-operated calcium entry: mechanisms and modulation. *Biochem Biophys Res Commun*. 2015; 460: 40–9.
52. **Ivanova H, Vervliet T, Missiaen L, *et al.*** Inositol 1,4,5-trisphosphate receptor-isoform diversity in cell death and survival. *Biochim Biophys Acta*. 2014; 1843: 2164–83.
53. **Bittremieux M, Bultynck G.** p53 and Ca (2 +) signaling from the endoplasmic reticulum: partners in anti-cancer therapies. *Oncoscience*. 2015; 2: 233–8.
54. **Camello-Almaraz C, Gomez-Pinilla PJ, Pozo MJ, *et al.*** Mitochondrial reactive oxygen species and Ca2 + signaling. *Am J Physiol Cell Physiol*. 2006; 291: C1082–8.
55. **Feissner RF, Skalska J, Gaum WE, *et al.*** Crosstalk signaling between mitochondrial Ca2+ and ROS. *Front Biosci (Landmark Ed)*. 2009; 14: 1197–218.
56. **Chaudhari N, Talwar P, Parimisetty A, *et al.*** A molecular web: endoplasmic reticulum stress, inflammation, and oxidative stress. *Front Cell Neurosci*. 2014; 8: 213.
57. **Sovolyova N, Healy S, Samali A, *et al.*** Stressed to death - mechanisms of ER stress-induced cell death. *Biol Chem*. 2014; 395: 1–13.